Current Topics in Biochemical Research
Vol. 9, *2*, 2007

Review

Enzymatic bioremediation: organophosphate degradation by binuclear metallo-hydrolases

Fernanda Ely[1,†], Jee-Loon Foo[2,†], Colin J. Jackson[2], Lawrence R. Gahan[1], David Ollis[2,b,*] and Gerhard Schenk[1,a,*]

[1]School of Molecular and Microbial Sciences, University of Queensland, St Lucia QLD 4072,
[2]Research School of Chemistry, Australian National University, Canberra ACT 0200, Australia

ABSTRACT

Organophosphate (OP) pesticides are used worldwide in agriculture, producing a market of around 30 billion dollars per year. Although OPs are highly toxic for humans, many bacteria are not affected by their presence, and some bacterial enzymes are able to hydrolyse OPs into non-toxic compounds. Of particular interest is the recent emergence of a number of phosphotriesterases (PTEs), especially in some bacteria found in soil, such as *Agrobacterium radiobacter* and *Pseudomonas diminuta*. These enzymes are binuclear metallohydrolases and are able to degrade a wide range of phosphotriesters, including various pesticides and nerve gas agents (e.g. sarin). Thus they have received attention for their potential use in detoxification of contaminated soil and water. Recently, a series of highly efficient β-lactamase-related methyl parathion hydrolases (MPHs) have been isolated from several bacterial strains. In addition, a glycerophosphodiesterase (GpdQ) discovered from *Enterobacter aerogenes* with activity towards stable aliphatic phosphodiesters as well as promiscuous activity towards phosphotriesters and phosphomonoesters has been characterised recently. These enzymes join the ranks of OP-degrading enzymes as potential bioremediation agents. Here, we will review the properties, functions and structures of these binuclear metallo-hydrolases, with focus on the well-characterised PTEs.

KEYWORDS: organophosphates, bioremediation, organophosphate degrading enzymes, binuclear metallohydrolases, phosphotriesterases, glycero-phosphodiesterase

1. INTRODUCTION

For over 4,500 years humans have been using pesticides to prevent crop damage. However, in the last 50 years the use of these compounds has increased dramatically, facilitating the development or expansion of agriculture in many regions of the world [1]. The pesticide industry generates a global market of around 30 billion dollars per year, with 2.5 million tons being used annually around the world [2]. However, the increasing use of pesticides has become a subject of growing concern due to their lasting toxic effects. The situation is alarming, especially in many developing countries, where the number of deaths caused by pesticide poisoning is higher than that caused by infectious diseases [3]. Pesticides are classified according to chemical functional groups, and one of the most widely and commonly used compounds are the organophosphates (OPs; Figure 1). Approximately 50,000 OPs are known to have some biological activity; the derivatives of major commercial and toxicological interest are esters or thiols derived from phosphoric, phosphinic

*Corresponding authors
[a]schenk@uq.edu.au
[b]ollis@rsc.anu.edu.au
[†]These authors contributed equally

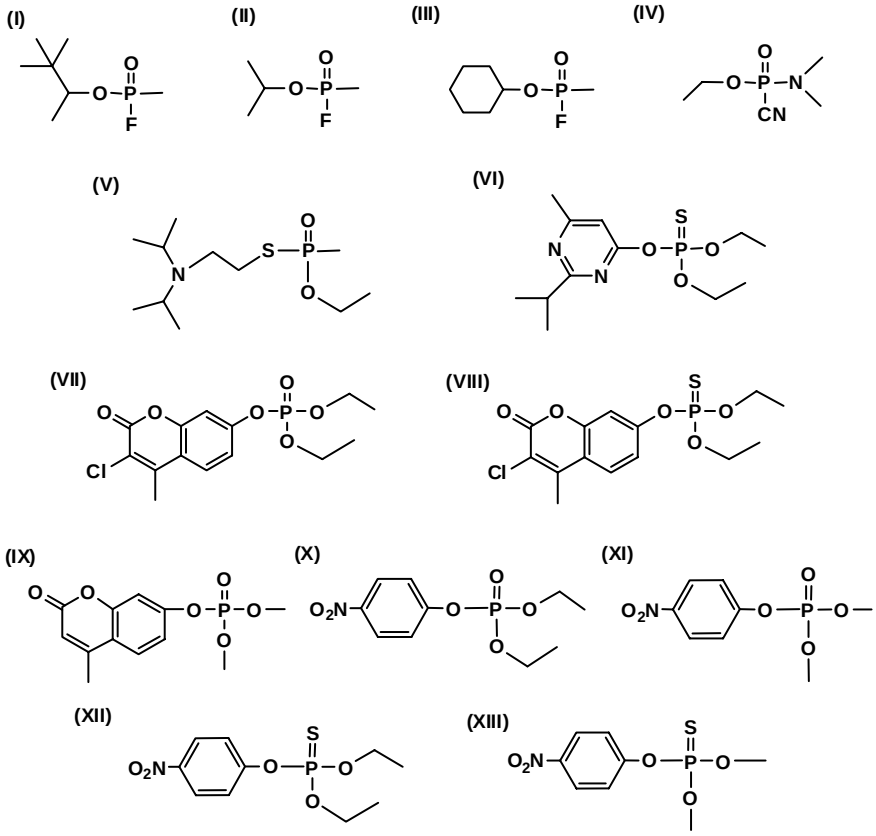

Figure 1. Structures of some OP compounds. (I) Soman; (II) sarin; (III) cyclosarin; (IV) tabun; (V) VX; (VI) diazinon; (VII) coroxon; (VIII) coumaphos; (IX) dMUP; (X) paraoxon; (XI) paraoxon-methyl; (XII) parathion; (XIII) methyl-parathion.

or phosphoramidic acids [4]. The most toxic OPs reported are the nerve agents tabun (GA), sarin (GB), cyclosarin (GF), soman (GD) and VX (Figure 1). These compounds have been used in chemical warfare and bioterrorism, and are currently classified as weapons of mass destruction by the United Nations. Their toxicity is ascribed mainly to their irreversible anti-cholinesterase activity, leading to the accumulation of acetylcholine and stimuli of nicotinic and muscarinic receptors [5].

OPs are synthetic chemicals and do not occur naturally. However, some bacterial organisms isolated from soil contaminated with OPs have recently evolved the ability to degrade (hydrolyse) many of these compounds. Several OP-degrading binuclear metalloenzymes have been isolated from these bacteria and the most thoroughly characterized of these are the phosphotriesterases (PTEs) from *Flavobacterium sp* ATCC 27551 [6], *Pseudomonas diminuta* [7] and *Agrobacterium radiobacter* [8]. The PTEs isolated from *Flavobacterium sp* ATCC 27551 and *P. diminuta* (OPH) were found to be identical while that extracted from *A. radiobacter* (OPDA) is closely related (~90% sequence identity) [8]. Recently, two enzymes with near-identical sequences have been isolated from *Plesiomonas* sp. strain M6 (*M6*MPH) [9] and *Pseudomonas* sp. WBC-3 (*WBC3*MPH) [10] which exhibit methyl-parathion hydrolase (MPH) activity. Subsequently, many other MPHs with high sequence identities were discovered from numerous strains of bacteria grown in soil contaminated with various OPs [11, 12, 13, 14]. These MPHs, however, share no significant homology with the PTEs. No naturally occurring substrates have yet been identified for the PTEs [15] but recent work suggests they have evolved from a family of bacterial lactonases [16]. The natural substrate for the MPHs is also

unknown, but on the basis of their similarity to the metallo-β-lactamases, it is believed they belong to, or have evolved from, the lactamase superfamily [17]. GpdQ, isolated from *Enterobacter aerogenes*, is primarily a phosphodiesterase and is known to degrade dimethyl and diethyl phosphate [18, 19]. This enzyme is part of the glycerol-3-phosphate uptake operon in *E. aerogenes* and its natural substrate is likely to be glycerolphosphoryl-ethanolamine, a typical phospholipid metabolite [20]. Although primarily a phosphodiesterase, GpdQ exhibits promiscuous phosphotriesterase activity [20, 21], illustrating the potential of this enzyme as a versatile and promiscuous phosphorolytic biocatalyst.

Owing to the chemical stability of OPs, they consequently tend to accumulate in the environment and thus become a significant biohazard. Traditional methods used for removal of OPs from contaminated soils and water, such as adsorption onto clay-based surfaces, are costly and often ineffective. A much more efficient and cost-effective method of removal is bioremediation. Field trials conducted using OPDA for large-scale decontamination of OPs strongly exemplifies the potential of OP-degrading enzymes as bioremediation and anti-biological warfare agents [22].

The enzymes discussed above are generally rather promiscuous with respect to substrate utilisation, and by means of directed evolution it has been shown mutants of OP-degrading enzymes can be made to target specific groups of pesticides. In this mini review we revisit major developments in our understanding of the structure, function and properties of these enzymes, and it is hoped that the reader may find this a stimulating article about a burgeoning area of biochemical research.

2. General catalytic properties of OP-degrading enzymes

OPH and OPDA are highly promiscuous and catalyse the hydrolysis of a wide range of OP substrates [15], including some of the highly toxic chemical warfare agents [6, 23]. For certain substrates, such as paraoxon and parathion, the hydrolysis rates are nearly diffusion-limited. These two PTEs have high sequence identity (~90%) with two significant differences: the addition of 20 amino acids at the C-terminus of OPDA, and three amino acids differences located in the substrate binding pocket (Arg254His, Tyr257His and Phe272Leu, OPDA/OPH) [24]. A number of mutations were introduced into OPDA to elucidate which of these variations are important for observed differences in substrates specificity [25]. Although the deletion of the C-terminus domain had no effect on kinetic properties, an increased stability of OPDA was observed [24]. The Tyr257His and Phe272Leu mutants of OPDA have a reduced k_{cat} for methyl-substituted substrates, thus resembling OPH [25]. The presence of a Tyr and Phe in positions 257 and 272, respectively, in wild-type OPDA reduces the size of the active site, thus facilitating optimal binding of substrates with short side chains [25]. This accounts for the higher turnover number for methyl-substituted substrates by OPDA compared to OPH while the values for ethyl-substituted substrates are quite similar in both enzymes (Table 1) [8]. PTEs were initially thought to natively contain a single Zn(II) in the active site [26] but recent analysis by atomic absorption spectroscopy and anomalous scattering suggests that at least native OPDA is a Zn(II)/Fe(II) enzyme [27]. PTEs are also catalytically active as binuclear Co(II), Cd(II), Mn(II) or Ni(II) substituted forms [28].

The substrate specificity of GpdQ has recently been examined. Other than its natural substrate, glycerolphosphorylethanolamine, GpdQ is able to hydrolyse a wide range of phosphotriesters, phosphodiesters, phosphomonoesters and phosphono-monoesters, including a close analogue of EA2192, the toxic hydrolysis product of VX [20, 21]. It was found that GpdQ hydrolyses phosphodiesters faster than their corresponding methylphosphonate analogues [21]. p-Nitrophenyl phosphate diesters are better substrates than the corresponding aliphatic alkyl phosphodiesters and phosphotriesters with p-nitrophenol as leaving group are processed more rapidly when they are methyl-substituted. Phosphomonoesterase activity has also been detected in GpdQ albeit at a low level.

*M6*MPH, *WBC3*MPH and a series of closely related MPHs have been isolated from bacteria strains from contaminated soil in China [9, 14]. Like the other OP-degrading enzymes mentioned, MPHs also have a wide substrate range and are

Table 1. Comparison between OPDA and OPH kinetic constants towards a number of OPs substrates.

Substrate	OPDA		OPH	
	K_m (μM)	k_{cat} (min^{-1})	K_m (μM)	k_{cat} (min^{-1})
Dimethyl-substituted				
Parathion-methyl	61.2±2.3	94.2±0.8	32.9±1.7	5.6±0.05
dMUP	66.0±9.1	81.7±9.1	46.7±4.2	20.5±2.3
Diethyl-substituted				
Parathion	92.6±6.4	21.9±2.0	50.6±12.2	23.5±0.2
Paraoxon	242±61	33.5±0.5	225±14	46.0±0.4
Coumaphos	8.3±1.8	12.4±0.6	21.4±6.0	14.1±2.6
Coroxon	15.9±1.9	22.7±0.1	25.3±1.3	39.5±5.3
Diazinon	51.9±4.5	65.2±6.7	54.2±5.4	56.5±2.9

able to hydrolyse, in addition to methyl parathion, other phosphorothioates and phosphorothiolates such as parathion, fenitrothion, profenofos, chlorpyrifos and triazophos [12, 13, 14, 29]. The kinetic properties of these MPHs have not been thoroughly characterised although it has been determined that *M6*MPH and *WBC3*MPH [10] are able to hydrolyse methyl parathion at near diffusion-limited rates ($k_{cat}/K_m \sim 10^6$ M^{-1} s^{-1}) [17, 30].

3. Structural characterisation of OP-degrading enzymes

The active sites of PTEs, GpdQ and MPHs all contain a binuclear metal centre and belong to the structurally diverse, large family of binuclear metallohydrolases [31], alongside ureases [32], purple acid phosphatases [33], Ser/Thr protein phosphatases [34], some metallo-β-lactamases [35] and nucleases [36]. OPH was the first PTE to be structurally characterised [37]. It exhibits α/β barrel fold akin to those of the amidohydrolase superfamily [38, 39]. Subsequently, a number of PTE structures with exogenous ligands such as diisopropyl methylphosphonate, triethyl phosphate, diethyl 4-methylbenzylphosphonate and diethyl 4-methoxyphenyl phosphate bound to the active site have been reported [10, 40]. More recently, the structures of GpdQ [41] and *WBC3*MPH [17] have been determined. GpdQ is folded as an α/β sandwich [41] resembling other phosphoesterases, such as purple acid phosphatase [21], while *WBC3*MPH is folded as a slightly different αβ/βα-sandwich, structurally similar to β-lactamases [17].

3.1. Overall structure

The overall structure of PTE was first determined from the apoform of OPH [37]. Subsequently, structures of several metal-substituted PTEs (Zn(II)/Zn(II), Zn(II)/Cd(II), Cd(II)/Cd(II), Mn(II)/Mn(II), Co(II)/Fe(II)) have been obtained [27, 37, 42]. All the structures show homodimers with folding typical of amidohydrolases [38, 39]. They are folded into a TIM barrel, which can be described as a distorted α/β barrel with eight parallel β-sheet strands forming the barrel, flanked on the outer surface by 14 α-helices [37, 43] (Figure 2). This α/β motif has been identified in a number of proteins, and represents a diverse structural family [44]. In some proteins this motif represents the majority of the structure (e.g. in triosephosphate isomerase [45]), while in others it forms just one domain of a multidomain structure, as observed for pyruvate kinase [46]. Reactions catalysed by such enzymes are as diverse as their tertiary structure, with some requiring co-factors (i.e. flavin, heme, [4Fe-4S] clusters, Mg(II) or

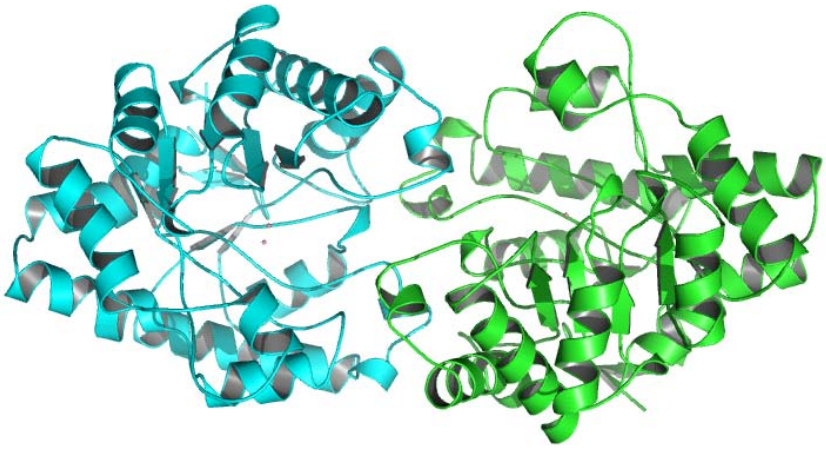

Figure 2. Overall structure of PTE. The dimeric structure of OPDA is shown with each subunit represented by a different color. PDB number: 2D2J.

Ca(II)) [43]. Despite this diversity, the catalytically relevant active sites in this structural family are generally located at the C-terminal end of the β-barrel [43]. Similarly, in PTEs the amino acids involved in metal ion coordination and substrate binding are clustered in the C-terminal portion of the barrel [42, 47]. Upon binding of metals in the active site of PTEs, numerous structural differences to the apoenzyme can be observed [37]. A superposition of the *α*-carbons of the structure of Cd(II)/Cd(II)-substituted OPH and those of the apoprotein results in a root-mean-square deviation (rmsd) of 3.4 Å. The most prominent variations in the backbone conformations of the two forms of PTE are located between residues Leu252 and Pro322 [47]. There is no significant conformational change between PTEs with different metal compositions apart from minor rearrangements in the metal binding site [37]. In each case, a carboxylated lysine residue (Lys169) has been identified as a metal ion-bridging ligand [43, 47]. Although OPH and OPDA share a high degree of similarity, with a rmsd of 0.38 Å [24], there are some structural differences between the proteins in their active sites, which will be discussed in the next section.

The structures of Zn(II)- and Co(II)-substituted GpdQ from *E. aerogenes* have recently been reported and show different folding in comparison to the PTEs [41]. While the PTEs form homodimers, GpdQ has a hexameric quaternary structure (a trimer of dimers) [42]. Each GpdQ dimer consists of three domains (Figure 3). The N-terminal domain (residues 1 - 195) forms a classic α/β-sandwich fold (seven β-sheets surrounded by five α-helices), and contains the metal ion-binding active site residues [41]. The central domain, labelled as "dimerization domain" (residues 196 - 255) is the main mediator for subunit interactions within a dimer via two-stranded β-sheets provided by each subunit [41]. The domain-swapped C-terminal section forms a helical extension that caps the α/β-sandwich in the N-terminal domain, thus narrowing the entrance to the active site [41]. GpdQ shows structural homology to various members of the family of metal-dependent phosphoesterases, with purple acid phosphatases being the closest relative [31, 33, 48, 49, 50]. A comparison of the α/β-sandwich domain of GpdQ and pig purple acid phosphatase demonstrated that the two proteins superimpose with a rmsd of 2.7 Å. Overall, it appears that GpdQ shares some structural features of both OP-degrading and purple acid phosphatase-like enzymes, which is consistent with a broad spectrum of substrates utilisable by this enzyme [21].

The structure of *WBC3*MPH that has been solved recently shows that the enzyme is structurally distinct from the PTEs (Figure 4) [17]. The MPH is a symmetrical 2-fold homodimer and each subunit is a β-lactamase-like domain consisting of an αβ/βα-sandwich in which three solvent-exposed α-helices flank two internal mixed

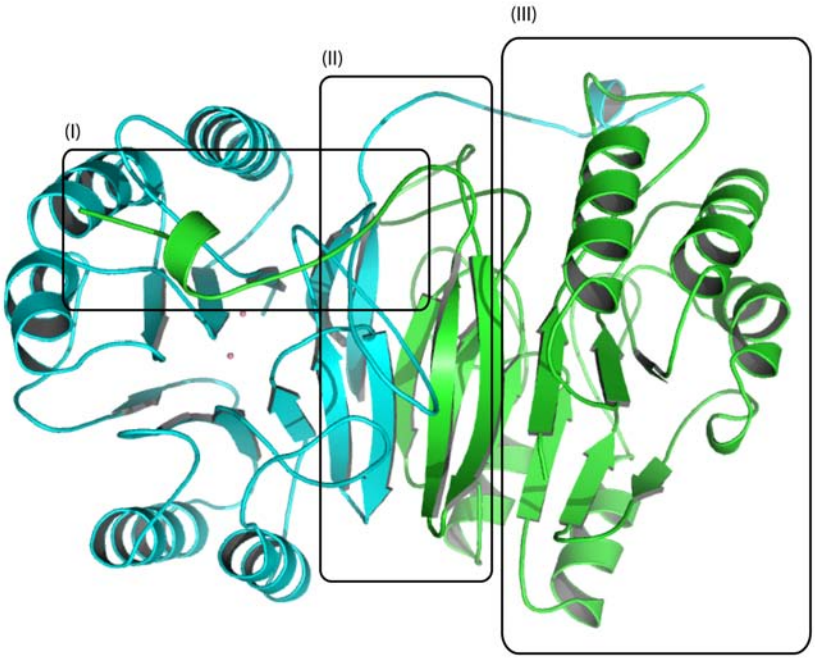

Figure 3. Structure of a dimeric GpdQ. The three domains and the metal binding site are represented: (I) "cap" domain (II) dimerization domain (III) α/β-sandwich domain. PDB number: 2DXN.

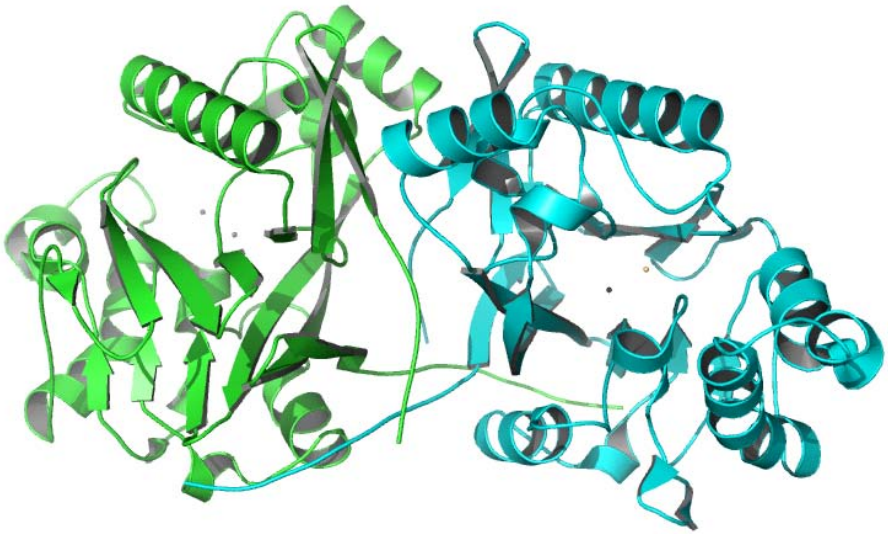

Figure 4. Structure of MPH. A cartoon representation of the homodimeric *WBC3*MPH. The monomers are shown in green and cyan. PDB number: 1P9E.

β-sheets [17]. Dimerization is facilitated by domain swapping between the N-terminal domain and a groove on the surface of the associated subunit and is believed to stabilise the metal binding centre [17]. Structurally, *WBC3*MPH is similar to the metallo-β-lactamases from *B. fragilis* and *S. maltophilia* and the β-lactamase domains of rubredoxin:oxygen oxidoreductase and human glyoxalase II with rmsd values between 1.4-1.6 Å [17].

3.2. Active-site structures

The PTEs have a binuclear metal centre located in the C-terminus of the β barrel, which provides four histidine residues as ligands (Figure 5a) [47]. For Cd(II)/Cd(II), Zn(II)/Cd(II) and Mn(II)/Mn(II) PTEs, the more buried metal site (α-site) is five-coordinate with a trigonal bipyramidal geometry formed by the four amino acids His55, His57, Asp301 and Lys169 and a hydroxide molecule. Both Lys169 and a hydroxide molecule act as bridges to the second more solvent-exposed metal site (β-site), which has additionally His201, His230 and two terminal water molecules as ligands, forming a distorted octahedral geometry [37, 47]. Co(II)/Fe(II) OPDA crystallised in the presence of poly(ethylene glycol) (PEG) has a similar structure except the α-metal adopts an octahedral geometry upon monodentate coordination of an ethylene glycol (EGL) molecule (Figure 5b), possibly from degradation of PEG [24]. In comparison, the β-metal ion of Zn(II)-substituted OPH adopts a five-coordinate, trigonal bipyramidal geometry, with one of the terminal water ligands moved away from Zn(II) into a non-coordinating position [37].

The protonation state of the bridging water molecule was probed in the Mn(II)-substituted form of OPH using EPR spectroscopy. At pH 8.3

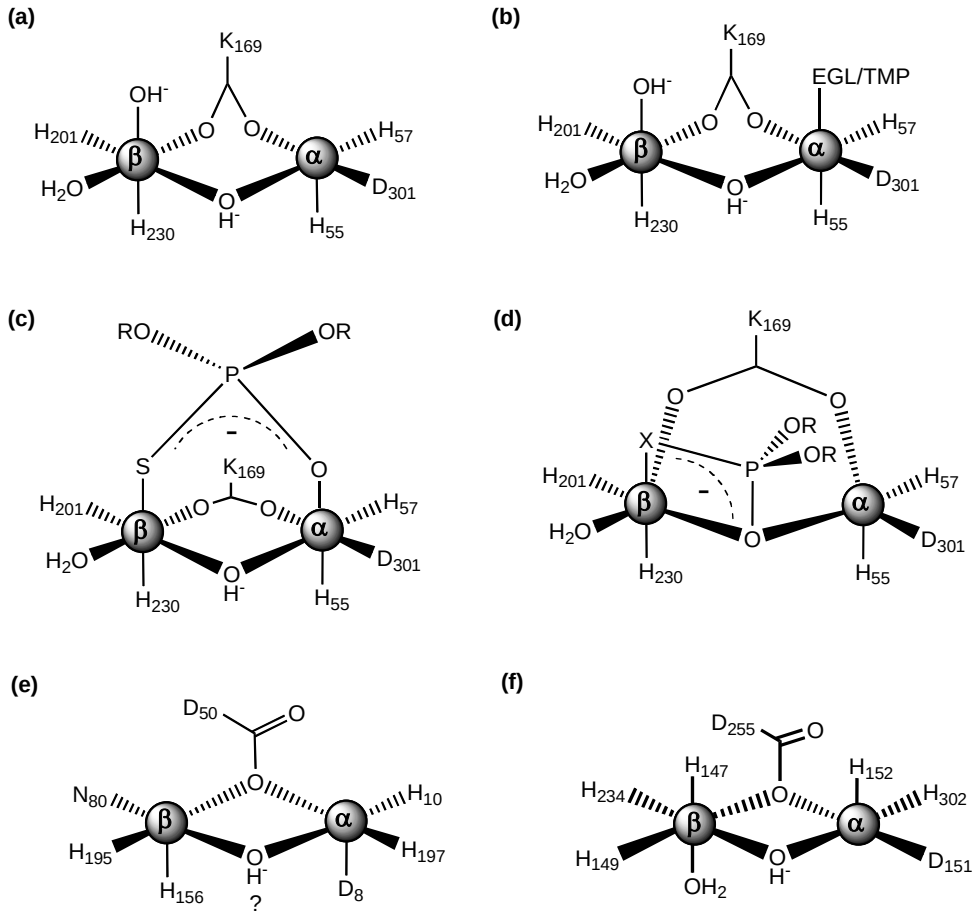

Figure 5. Metal coordination of PTEs and GpdQ. (a) Co(II)-substituted OPDA, Mn(II)-, Cd(II)- or Zn(II)/Cd(II)-substituted OPH (b) Co(II)-substituted OPDA complexed with EGL or TMP (c) Co(II)-substituted OPDA complexed with DMTP (R=Me) and DETP (R=Et) upon co-crystallisation with dimethoate and TEDTPP respectively (d) Co(II)-substituted OPDA complexed with exogenous DMTP (R=Me, X=S), DETP (R=Et, X=S) and DEP (R=Et, X=O) via co-crystallisation. (e) Zn(II)- or Co(II) substituted GpdQ (f) Zn(II)/Cd(II)-substituted *WBC3*MPH.

the spectral data are consistent with the presence of a μ-hydroxide (as evidenced from the relatively weak exchange coupling constant $|J| = 2.7 \pm 0.02$ cm^{-1}); decreasing the pH to 7.0 leads to its protonation, forming uncoupled Mn(II) species [51]. Molecular simulation studies, including *ab initio* and density functional theory calculation, with Cd(II)- and Zn(II)-substituted OPH have also demonstrated that a μ-hydroxide is present in the catalytically active enzyme [52, 53]. Additionally, the metal ions are also bridged by the carboxylated Lys169 (Figure 5a), where the carboxylic oxygens are directly interacting with the metal ions. This covalent modification of the Lys residue has also been observed for a number of other enzymes, including a urease from *Klebsiella aerogenes* [32], a class D β-lactamase from *P. aeruginosa* [54] and a ribulose-1,2-bisphosphate carboxylase from spinach [55].

The structure of PTE was also investigated in the presence of a number of substrate analogues, including diisopropyl methyl phosphonate (DMP), triethyl phosphate (TEP), diethyl 4-methyl-benzylphosphonate (DMBP) [40], trimethyl phosphate (TMP) [42] and diethyl 4-methoxyphenyl phosphate (EPO) [10]. The binding of these compounds defines a rather large substrate binding pocket in the vicinity of the binuclear centre, providing an explanation for the large range of substrates that can be hydrolysed by this enzyme. The overall structure of PTE is not greatly affected by the interaction with these analogues. With the exception of TMP, which binds to the α-metal via the phosphoryl oxygen (Figure 5b), the other analogues coordinate to, or are bound in the vicinity of the β-metal resulting in some structural rearrangements at that site. An oxygen atom of the phosphoryl group of DMP, a sarin analogue, is coordinated to the β-zinc (2.5 Å), while none of TEP, DMBP or EPO directly interacts with the metal ion in the β-site [40]. In the DMP-bound structure Zn(II) in the β-site retains a distorted trigonal bipyramidal geometry, where the phosphoryl oxygen of the inhibitor replaces the terminal H_2O. In contrast, in TEP-DMBP- and EPO-bound complexes the β-site adopts tetrahedral geometry, with the β-metal coordinated by His201, His230, Lys169 and the μ-hydroxide; no terminal water ligand is present [40]. Unlike DMBP, which binds in a non-productive mode, EPO is oriented such that the phenolic leaving group is pointing towards the solvent and interacting with the aromatic residues in the leaving group channel (Trp131, Phe132, Phe306 and Tyr309). This structure is particularly noteworthy as EPO is structurally very similar to paraoxon, a highly favoured substrate; hence, the binding orientation of EPO is likely to depict substrate binding more accurately than other reported PTE-inhibitor structures [10].

Apart from substrate analogues, structures of hydrolysis products bound in PTE have also been studied. Dimethyl thiophosphate (DMTP) and diethyl thiophosphate (DETP) generated from the hydrolysis of dimethoate and tetraethyl dithiopyrophosphate (TEDTPP), respectively, bind bidentately in a μ-1,3 fashion to the α- and β-sites, via the ligands' oxygen and sulfur atoms, respectively (Figure 5c) [10, 42]. Due to the concomitant expulsion of a terminal water ligand the β-site is five-coordinate with a trigonal-bipyramidal geometry [42]. Interestingly, when PTE crystals were soaked with DETP, the molecule chelated the β-metal and bridged the two metal sites in a μ-1,1 fashion via the oxygen atom, displacing the bridging hydroxide in the process (Figure 5d) [10]. In this structure, both metal sites assumed trigonal bipyramidal geometry [10].

In PTE, three distinct regions (subsites) within the substrate binding pocket have been identified, termed the leaving group, small and large subsite [24, 47]. The residues within the leaving group and small subsites are identical in both OPH and OPDA and are Trp131, Phe132, Phe306 and Tyr309, and Gly60, Ile106, Leu303 and Ser308, respectively. In the large subsite, Arg254 and Tyr257 in OPDA are replaced by histidines in OPH; the remaining residues in this site, Leu271 and Met317, are conserved [24]. The leaving group channel is lined by a cluster of aromatic residues Trp131, Phe132, Phe306 and Tyr309. These have been observed in the PTE-EPO structure to interact extensively with the aromatic leaving group, hence suggesting the facilitation of substrate binding by these amino acids [10].

The differences between OPH and OPDA in the large subsite of the substrate pocket are believed to be the underlying cause for the observed variation in substrate specificity between these two enzymes. Specifically, crystal structures of

OPDA in the absence or presence of DMTP illustrate the importance of Arg254 in substrate binding. In the absence of this analogue Arg254 appears to point away from the active site, but undergoes a structural rearrangement upon addition of the analogue, (i) displacing two unbound water molecules in the active site, and (ii) forming a hydrogen bond with a side chain oxygen atom of the analogue [42]. The latter is proposed to be important to both orient and stabilise the substrate molecule in the active site [42]. Substrate specificity in OPDA was also investigated using site-directed mutagenesis [25]. In particular, residues Arg254 and Tyr257 were replaced by histidines, thus mimicking the OPH large subsite. Despite its apparent involvement in substrate binding, replacement of Arg254 by a histidine does not affect substrate specificity significantly. In contrast, the Tyr257His mutant displays increased activity towards ethyl substituted substrates, while the activity for methyl substituted substrates is reduced. The substitution of Phe272, another residue in the vicinity of the large subsite, by a leucine leads to a similar effect [25]. This observation is not unexpected since replacement of the bulky tyrosine and phenylalanine residues by smaller histidines and leucine is anticipated to expand the large binding pocket of OPDA, thus improving access for ethylated substrates.

The first coordination sphere of the binuclear metal centre of GpdQ is shown in Figure 5e [41]. The α-metal is coordinated by His10, His197, Asp8 and Asp50, with the latter acting as a μ-1,1 bridge between the two metal ions. Due to the limited resolution of the GpdQ structure (2.9 Å) the presence or absence of a hydroxide/water bridge has not yet been verified [41]. The β-metal coordination sphere is completed by His195, Asn80 and His156 [41]. Substitution of Zn(II) by Co(II) does not lead to any significant structural differences. An anomalous scattering analysis has indicated that the more buried α-site has higher metal ion affinity than the more solvent exposed β-site [41], a feature that appears to be common to many members of the family of binuclear metallohydrolases [31, 56]. Specifically, the GpdQ active site is very similar to that of purple acid phosphatases (PAP), with the exception that His10 is replaced by a Tyr in the latter [31]. No substrate-bound structure of GpdQ is yet available and the binding mode of the substrate could involve bidentate or terminal coordination to the β-site.

The binuclear metal centre of MPH, based on the structure of *WBC3*MPH, is situated between two β-sheets and surrounded by two α/β-loops [17]. The bound metal has been determined to be zinc but the electron density map for the crystal shows that the two metals in the active site in each subunit are different [17]. It was found that because of the presence of $CdCl_2$ (an essential component for crystallisation) Zn^{2+} was displaced by Cd^{2+} at the more solvent exposed β-metal site [17]. In the reported structure, the two metal binding sites are bridged by a water molecule and Asp255. In addition to these ligands, the α-metal is coordinated by Asp151, His152 and His302 while the β-metal is bound by His147, His149, His234 and a terminal water (Figure 5f) [17]. The binding site is hydrophobic and is formed by hydrophobic residues including Leu65, Leu67, Phe119, Trp179, Phe196, Leu273 and Leu258 [17]. Both metal centres are six coordinate [17]. Considering the MPH's efficiency in hydrolysing methyl-parathion, which has an aromatic leaving group, it was suggested that the aromatic residues Phe119, Trp179 and Phe196 might be involved in substrate binding [17]. This hypothesis is supported by results from kinetic studies of mutants with single substitutions at these sites [17].

Although the PTEs, MPHs and GpdQ share no significant structural homology, their active sites share certain similarities. Their binuclear metal centres are likely to be bridged by a μ-hydroxide and contain several aspartate and several histidine metal ligands. The metal ions in GpdQ and MPH are additionally bridged by an asparatate, while a carboxylated lysine bridges the metals in the PTEs [17]. Both PTE and MPH have extremely hydrophobic binding sites with aromatic residues lining the entrance to the active site. In contrast, the binding site of GpdQ is more charged, consistent with its primary phosphodiesterase function.

4. Proposed reaction mechanisms for OP-degrading enzymes

The chemical mechanism for OP hydrolysis catalysed by PTE has been extensively studied by

a number of enzymological, structural and spectroscopic techniques. In OPH the two metal ions required for enzymatic activity bind cooperatively to the active site of the apoenzyme during the self-assembly of the binuclear centre [57]. Experiments in ^{18}O water and a chiral thiophosphonate substrate have shown that the cleavage of the P-O bond occurs via an S_N2 mechanism [58]. The rate-limiting step of the OPH reaction seems to depend on the substrate. Hydrolysis of less reactive substrates (with leaving groups $pK_a > 7.0$) is slower and limited by the P-O bond cleavage, while more reactive substrates (with leaving groups $pK_a < 7.0$) are turned over faster with a physical step, such as a conformational change or diffusion, limiting the overall rate [59]. A theoretical study using *ab initio* calculations has indicated that the chemical nature of the substrate may indeed affect the molecular mechanism of hydrolysis [60]. Specifically, with the highly labile 'fast' substrates PTE employs an S_N2-type mechanism in which chemical hydrolysis is not rate-limiting while with the 'slower' substrates decomposition of a pentacoordinate intermediate makes chemical hydrolysis rate-limiting [60].

The pH dependence of the k_{cat} indicates that (i) only one protonation equilibrium of the OPH-substrate complex, pK_a(ES), is relevant for catalysis, and (ii) the enzyme is most active in its deprotonated form [58]. Since pK_a(ES) depends on the identity of the metal ions in the binuclear centre, the residue associated with this protonation equilibrium is expected to be bound to at least one of the two metal ions. Structural and EPR pH dependent studies of OPH [40, 51] identify the μ-hydroxide bridge as the likely candidate residue, leading to the suggestion that this group is the reaction-initiating nucleophile. The proposed reaction mechanism for OPH-catalysed OP hydrolysis is shown in Figure 6. The substrate is bound in a monodentate fashion to the β-metal in the active site followed by a nucleophilic attack from the μ-hydroxide with the assistance of His254 and Asp233 in proton-shuttling. A recent theoretical study on the active site of PTE has proposed that binding of the phosphoryl oxygen of the substrate to the β-metal weakens the bond between the β-metal and the μ-hydroxide [61]. This bond weakening results in a pseudo-monodentate coordination of this hydroxide to the α-metal ion, thus increasing its nucleophilicity. A similar shift of the bridging hydroxide towards a pseudo-monodentate coordination has been observed in PAPs upon addition of substrates and substrate analogues [31, 62, 63, 64]. Upon hydrolysis of the substrate it is proposed that the phosphodiester product remains bound to the active site in a μ-1,3 mode before being released and the active site is regenerated [65].

Recent structures of OPDA with bound hydrolysis products have provided evidence for an alternative mechanism with crystal soaking of OPDA with dimethoate and TEDTPP yield hydrolysis products (DMTP and DETP, respectively) binding in μ-1,3 mode to the metal ions with the bridging hydroxide still present [10, 42]. However, exogenous DETP and DEP bind by chelating to the β-metal with the oxygen bridging the metal ions in μ-1,1 fashion, displacing the bridging hydroxide (Figure 5d) [61]. This suggests that the hydrolysis products captured in a μ-1,3 binding mode is the conformation assumed immediately after nucleophilic attack [10, 42], followed by a rearrangement of the diester product to coordinate in a μ-1,1 binding mode, thus displacing the bridging hydroxide. Hence, an α-metal-bound terminal hydroxide is proposed to be the initiating nucleophile instead of the bridging hydroxide (Figure 7) [10, 42]. This hypothesis is supported by comparing molecular dynamics docking results with the structure of the OPDA-EPO complex [10], in which the alignment of the substrate favours nucleophilic attack from a terminal nucleophile. It is proposed that the catalytic role of bridging hydroxide in PTE is to function as a general base to deprotonate a terminal water to act as a nucleophile (Figure 7). This mechanism may reconcile previous spectroscopic results with the findings from the recent crystal structures as it confirms the protonation state of the μ-hydroxo bridge will be essential to catalysis.

GpdQ is a rather promiscuous phosphoesterase, with a preference for diester substrates, but considerable reactivity towards a number of mono- and triesters [18, 20, 21]. Importantly,

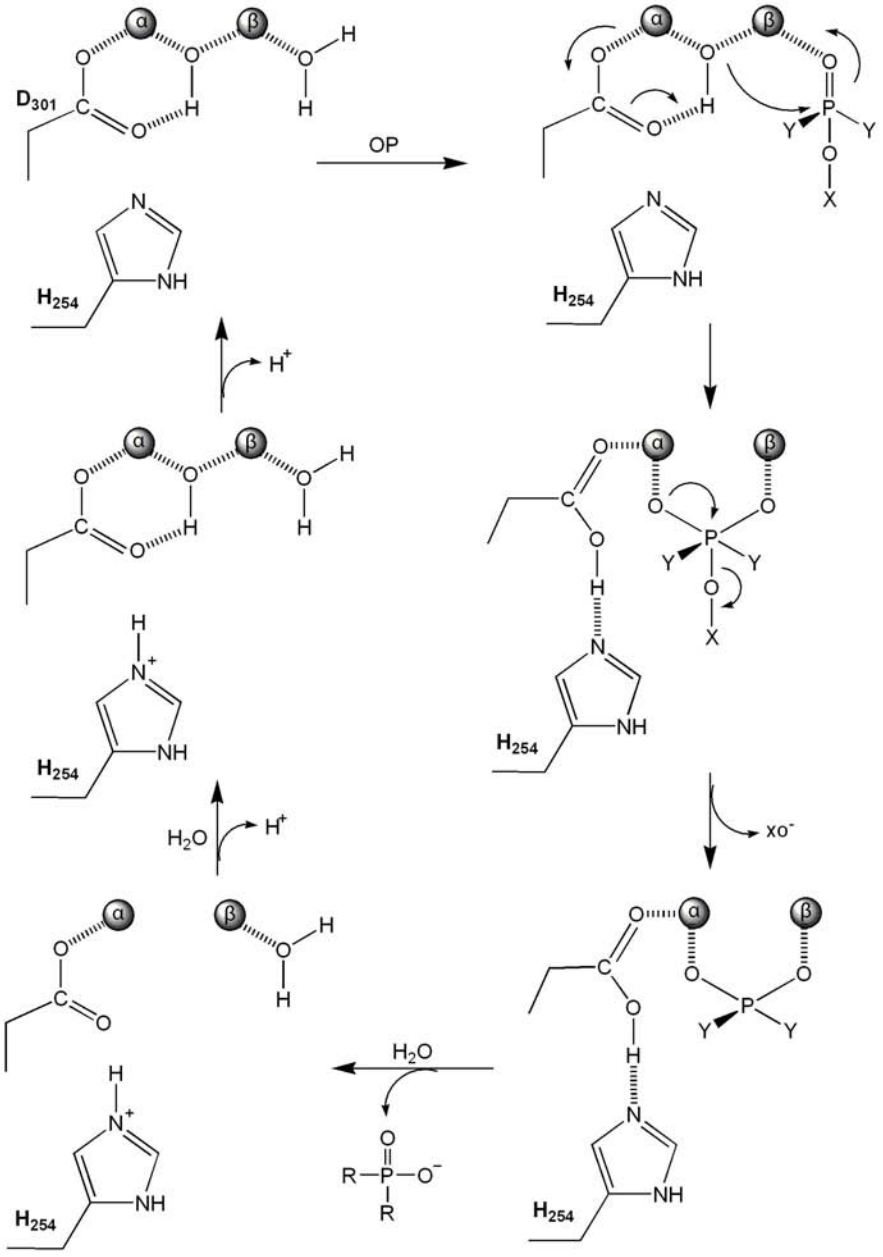

Figure 6. Proposed catalytic mechanism for OPH using the μ-hydroxo ligand as nucleophile. The substrate is activated via P-O bond polarisation upon binding to the β-metal. The bridging hydroxide attacks the electrophilic phosphorus with the assistance of a proton relay system. A pentacoordinated intermediate is formed. Upon departure of the hydrolysis products, the active site is regenerated, by forming a μ-hydroxo bridge.

GpdQ is able to hydrolyse the O-ethyl analogue of EA 2192, the most toxic degradation product of the nerve agent VX [21]. Furthermore, like OPDA, GpdQ appears to prefer methyl- over ethyl-substituted substrates [21]. In the absence of mechanistic and structural data the molecular details of the GpdQ-catalysed reaction cycle remain obscure. However, due to the similarities between the active site structures of GpdQ and a number of binuclear metallohydrolases, notably PAPs, it is envisaged that these enzymes also employ a similar mechanism [18, 31, 66].

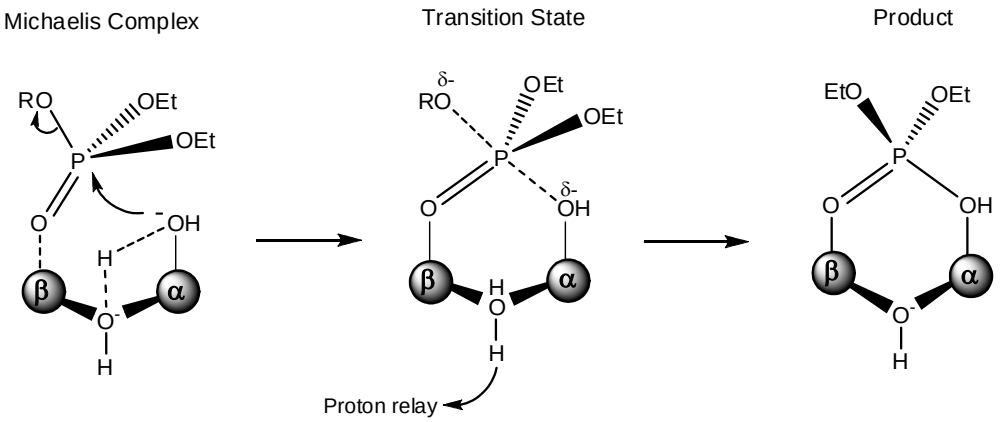

Figure 7. Proposed catalytic mechanism for OPDA using a terminal hydroxide nucleophile and the μ-hydroxo ligand as general base. The uncharged substrate is loosely bound to the β-metal. A water molecule interacts with the α-metal and the μ-hydroxo bridge, thus lowering its pK_a and generates a hydroxide nucleophile terminally bound to the α-metal, ideally aligned to attack the electrophilic phosphorus. A proton relay system shuttles the proton away from μ-hydroxo bridge and the active site. After leaving group departure, the phosphodiester product bridges the metal ions and the μ-hydroxo bridge remains intact.

No mechanistic study has been performed with MPH. However, since its active site shares structural features with PTEs, its catalytic mechanism is anticipated to resemble those reported for OPH (Figure 6) or OPDA (Figure 7). Accordingly, the substrate, methyl-parathion, is likely to coordinate to the β-metal via the thiophosphoryl sulphur, and nucleophilic attack most probably occurs from a solvent molecule activated through its interaction with the α-metal ion.

5. Directed evolution: an approach to develop optimised bioremediator

Techniques for the rational design of proteins are widely used and are powerful tools to explore reaction mechanisms of enzymes and to improve enzyme function [67]. The stereoselectivity of OPH towards chiral substrates, for example, was investigated using site-directed mutagenesis [68, 69, 70, 71]. Mutagenesis has also been employed to improve and/or evolve enzymatic activity [72], specificity [73], stability [74], and/ or solubility [75]. Directed evolution involves a library of mutants of the target gene, created by using random mutagenesis and/or gene recombination [76, 77, 78]. From this library, mutants with improved desired properties (e.g. altered substrate specificity, increased turnover rate, etc.) are selected by high-throughput screening methods (for an extensive review of methods and applications see reference 79). The ability of OPH and OPDA to degrade OPs makes these enzymes promising systems for the evolution of detoxification agents [80] with enhanced catalytic activity towards specific OP pesticides and nerve gas agents [15]. The enzymatic decomposition of toxic OPs accumulated in contaminated water and soil is a potent avenue for bioremediation, and may also play an important role as an antibiological warfare strategy [81, 82]. Due to the catalytic efficiency and specificity enzymatic bioremediation is anticipated to be far more practical and cheaper than other means for removing OPs. This has been demonstrated in field trials conducted using OPDA as a bioremediation agent [22]. The success of these experiments subsequently led to the commercialisation of bioremediation formulas containing OPDA under the brand name LandGuard™ by Orica Water (Melbourne, Vic., Australia) [27].

In general, while the generation of mutant libraries does not pose a major problem, the selection of mutants with improved desired properties is more challenging. The simplest method is to select bacterial colonies via plate assay based on the size of the haloes formed as a result of substrate

hydrolysis. This method has been used for identifying mutants with enhanced activities towards methyl-paraoxon and chlorpyrifos [83, 84]. An innovative system based on *in vitro* compartmentalisation (IVC) was also employed to isolate a variant OPH with a 63-fold increase in k_{cat} for paraoxon [85]. Mutant genes are bound to microbeads, compartmentalised in a water-in-oil emulsion and translated *in vitro* [85]. A paraoxon analogue is added to the emulsion, followed by a fluorescent tag which binds to the microbead-anchored hydrolysis product [85]. The beads are then sorted by flow cytometry based on the microbeads' fluorescence [85]. Recently, a number of fluorogenic analogues of OPs with a 3-chloro-7-oxy-4-methylcoumarin leaving group were developed as probes for high-throughput screening [86]. This series of compounds includes analogues of the pesticides paraoxon, parathion and dimefox, and the nerve agents sarin, cyclosarin, soman, VX, Russian-VX, tabun and diisopropyl fluorophosphate. Coupling these substrates with IVC in a water-in-oil-in-water double emulsion would allow rapid screening of mutant libraries by fluorescence-activated cell sorting [85]. This method is more efficient and effective since the need for an additional fluorescent marker and a highly modified substrate to produce a microbead-bound hydrolysis product is eliminated [87].

An alternative screening method for OPDA mutants was recently developed by our group [20, 88]. *Escherichia coli* (strain DH10B) is unable to grow on medium that contains paraoxon as sole source for phosphorous. However, when GpdQ and OPDA are coexpressed in *E. coli*, the strain acquires the ability to grow in medium that only contains paraoxon as phosphorous source [20]. While OPDA degrades the OP, GpdQ further hydrolyses the diester product of the OPDA-catalysed reaction to a monoester [21]. The monoester is then hydrolysed into inorganic phosphate, the nutrient required in cell metabolism, by a monoesterase (e.g. alkaline phosphatase). This modified *E. coli* strain has already been successfully used to select for OPDA mutants with increased expression levels [88], and is currently being employed to screen for OPDA mutants with altered substrate specificities. A recent study has shown that the cell growth rate using this system is dependent on the expression level of the PTE mutant, and the rates of hydrolysis of the OP and the phosphodiester product by PTE and GpdQ, respectively [21].

6. CONCLUSIONS

PTEs and MPHs are highly efficient OP-degrading enzymes. Their surprisingly high activity towards, and broad substrate specificity for a large range of OPs make them good candidates to be developed (i) into versatile bioremediators for contaminated soils and water, and (ii) as anti-warfare agents. Of the two classes of enzymes, only the former has been well-characterised. These binuclear metalloenzymes are able to operate with a range of different divalent metal ions, including Fe(II), Mn(II), Co(II), Cd(II) and Ni(II), with no or moderate changes in reactivity. Kinetic, structural and spectroscopic studies with a variety of metal ions and inhibitors have been carried out, especially with OPH, which have provided detailed insight into the reaction mechanism(s) of these enzymes. Although structurally very similar, OPDA and OPH differ with respect to their preferred substrates. OPDA has a significantly higher turnover rate for methyl-substituted substrates, while the activity towards ethyl-substituted substrates is similar for both enzymes. Various diester products of PTE catalysed reactions can be further hydrolysed by GpdQ, a highly promiscuous phosphodiesterase. Interestingly, the crystal structure of GpdQ indicates that its active site has a binuclear metal centre similar to that of several members of the family of binuclear phospho-monoesterases, notably the PAPs. Although natively a glycerophosphodiesterase, its practical significance is linked to its complementarity to the OP-degrading enzymes, and its potential to be engineered into an improved OP hydrolase.

ACKNOWLEDGEMENTS

This work was funded by a grant from the Australian Research Council (DP0664039).

7. REFERENCES

1. Miller, G. T. Jr. 2002, Living in the environment (12th Ed.). Belmont: Wadsworth/Thomson Learning.
2. McKenzie, W. 2001, Agrochemical service: the world market in 2000. In: Annual review of the crop protection association. Peterborough: Crop Protection Association.

3. Eddleston, M., Karalliedde, L., Buckley, N., Fernando, R., Hutchinson, G., Isbister, G., Konradsen, F., Murray, D., Piola, J. C., Senanayake, N., Sheriff, R., Singh, S., Siwach, S. B., and Smit, L. 2002, Lancet, 360, 1163.
4. Sogorb, M. A., and Vilanova, E. 2002, Toxicol. Lett., 128, 215.
5. Kamanyire, R., and Karalliedde, L. 2004, Occup. Med., 54, 69.
6. Sethunathan, N., and Yoshida, T. 1973, Can. J. Microbiol., 19, 873.
7. Munnecke, D. M. 1976, Appl. Environ. Microbiol., 32,7.
8. Horne, I., Sutherland, T. D., Harcourt, R. L., Russell, R. J., and Oakeshott, J. G. 2002, Appl. Environ. Microbiol., 68, 3371.
9. Zhongli, C., Shunpeng, L., and Guoping, F. 2001, Appl. Environ. Microbiol. 67, 4922.
10. Jackson, C. J., Foo, J-L., Kim, H-K., Carr, P. D., Liu, J-W., Salem, G., and Ollis, D. L. 2008, J. Mol. Biol., 375, 1189.
11. Zhang, R., Cui, Z., Jiang, J., He, J., Gu, X., and Li, S. 2005, Can. J. Microbiol., 51, 337.
12. Zhang, Z., Hong, Q., Xu, J., Zhang, X., and Li, S. 2006, Biodegradation, 17, 275.
13. Li, X., He, J., and Li, S. 2007, Res. Microbiol., 158, 143.
14. Liu, H., Zhang, J-J., Wang, S-J., Zhang, X-E., and Zhou, N-Y. 2005, Biochem. Biophys. Res. Commun., 334, 1107.
15. Raushel, F. M. 2002, Curr. Opin. Microbiol., 5, 288.
16. Afriat, L., Roodveldt, C., Manco, G., and Tawfik, D. S. 2006, Biochemistry, 45, 13677.
17. Dong, Y. J., Bartlam, M., Sun, L., Zhou, Y. F., Zhang, Z. P., Zhang, C. G., Rao, Z., and Zhang, X. E. 2005, J. Mol. Biol., 353, 655.
18. Gerlt J. A., and Whitman G. J. R. 1975, J. Biol. Chem., 250, 5053.
19. Gerlt, J. A., and Westheimer, F. H. 1973, J. Am. Chem. Soc., 95, 8166.
20. McLoughlin, S. Y., Jackson, C., Liu, J-W., and Ollis, D. L. 2004, Appl. Environ. Microbiol., 70, 404.
21. Ghanem, E., Li, Y., Xu, C., and Raushel, F. M. 2007, Biochemistry, 46, 9032.
22. Sutherland, T. D., Horne, I., Weir, K. M., Coppin, C. W., Williams, M. R., Selleck, M., Russell, R. J., and Oakeshott, J. G. 2004, Clin. Exp. Pharmacol. Physiol., 31, 817.
23. Raushel, F. M., and Holden, H. M. 2000, Adv. Enzymol. Relat. Areas Mol. Biol., 74, 51.
24. Yang, H., Carr, P. D., McLoughlin, S. Y., Liu, J. W., Horne, I., Qiu, X., Jeffries, C. M. J., Russell, R. J., Oakeshott, J. G., and Ollis, D. L. 2003, Protein Eng., 16, 135.
25. Horne, I., Qiu, X., Ollis, D. L., Russell, R. J., and Oakeshott, J. G. 2006, FEMS Microbiol. Lett., 259, 187.
26. Dumas, D., Caldwell, S., Wild, J., and Raushel, F. 1989, J. Biol. Chem., 264, 19659.
27. Jackson, C., Carr, P. D., Kim, H. K., Liu, J-W., Herrald, P., Mitic, N., Schenk, G., Smith, C. A., and Ollis, D. L. 2006, Biochem. J., 397, 501.
28. Omburo, G., Kuo, J., Mullins, L., and Raushel, F. 1992, J. Biol. Chem., 267, 13278.
29. Dai, Q., Zhang, R., Jiang, J., Gu, L., and Li, S. 2005, Acta Pedologica Sinica, 42, 111.
30. Xue, W., Liu, W., Li, S., Cui, Z., and Lin, H. 2006, High Technology Letters, 16, 84-87.
31. Mitić, N., Smith, S. J., Neves, A., Guddat, L. W., Gahan, L. R., and Schenk, G. 2006, Chem. Rev., 106, 3338.
32. Jabri, E., Carr, M. B., Hausinger, R. P., and Karplus, P. A. 1995, Science, 268, 998.
33. Schenk, G., Gahan, L. R., Carrington, L. E., Mitić, N., Valizadeh, M., Hamilton, S. E., de Jersey, J., and Guddat, L. W. 2005, Proc. Natl. Acad. Sci. USA, 102, 273.
34. Jin, H., and Pancholi, V. 2006, J. Mol. Biol., 357, 1351.
35. Crisp, J., Conners, R., Garrity, J. D., Carenbauer, A. L., Crowder, M. W., and Spencer, J. 2007, Biochemistry, in press.
36. Devos, J. M., Tomanicek, S. J., Jones, C. E., Nossal, N. G., and Mueser, T. C. 2007, J. Biol. Chem., in press.
37. Benning, M. M., Shim, H., Raushel, F. M., and Holden, H. M. 2001, Biochemistry, 40, 2712.
38. Holm, L., and Sander, C. 1997, Proteins: Struct. Funct. Genet., 28, 72.
39. Seibert, C. M., and Raushel, F. M. 2005, Biochemistry, 44, 6383.
40. Benning, M. M., Hong, S-B., Raushel, F. M., and Holden, H. M. 2000, J. Biol. Chem., 275, 30556.

41. Jackson, C. J., Carr, P. D., Liu, J. W., Watt, S. J., Beck, J. L., and Ollis, D. L. 2007, J. Mol. Biol., 367, 1047.
42. Jackson, C., Kim, H. K., Carr, P. D., Liu, J. W., and Ollis, D. L. 2005, Biochim. Biophys. Acta, 752, 56.
43. Benning, M. M., Kuo, J. M., Raushel, F. M., and Holden, H. M. 1994, Biochemistry, 33, 15001.
44. Efimov, A. V. 1997, Proteins, 28, 241.
45. Casteleijn, M. G., Alahuhta, M., Groebel, K., El-Sayed, I., Augustyns, K., Lambeir, A-M., Neubauer, P., and Wierenga, R. K. 2006, Biochemistry, 45, 15483.
46. Valentini, G., Chiarelli, L. R., Fortin, R., Dolzan, M., Galizzi, A., Abraham, D. J., Wang, C., Bianchi, P., Zanella, A., and Mattevi, A. 2002, J. Biol. Chem., 277, 23807.
47. Benning, M. M., Kuo, J. M., Raushel, F. M., and Holden, H. M. 1995, Biochemistry, 34, 7973.
48. Sträter, N., Klabunde, T., Tucker, P., Witzel, H. and Krebs, B. 1995, Science, 268, 1489.
49. Knöfel, T., and Sträter, N. 1999, Nat. Struct. Biol., 6, 448.
50. Guddat, L. W., McAlpine, A. S., Hume, D., Hamilton, S., de Jersey, J., and Martin, J. L. 1999, Structure, 7, 757.
51. Samples, C. R., Howard, T., Raushel, F. M., and DeRose, V. J. 2005, Biochemistry, 44, 11005.
52. Zheng, F., Zhan, C-G., and Ornstein, R. L. 2002, J. Phys. Chem. B, 106, 717.
53. Krauss, M. 2001, J. Chem. Inf. Comput. Sci., 41, 8.
54. Li, J., Cross, J. B., Vreven, T., Meroueh, S. O., Mobashery, S., Schlegel, H. B. 2005, Proteins, 61, 246.
55. Maveyraud, L., Golemi, D., Kotra, L. P., Tranier, S., Vakulenko, S., Mobashery, S., and Samama, J. P. 2000, Structure Fold. Des., 8, 1289.
56. White, D. J., Reiter, N. J., Sikkink, R. A., Yu, L., and Rusnak, F. 2001, Biochemistry, 40, 8918.
57. Shim, H., and Raushel, F. M. 2000, Biochemistry, 39, 7357.
58. Lewis, V. E., Donarski, W. J., Wild, J. R., and Raushel, F. M. 1988, Biochemistry, 27, 1591.
59. Caldwell, S. R., Newcomb, J. R., Schlencht, K. A., and Raushel, F. M. 1991, Biochemistry, 30, 7438.
60. Jackson, C., Liu, J. W., Coote, M. L., and Ollis, D. L. 2005, Org. Biomol. Chem., 3, 4343.
61. Chen, S. L., Fang, W. H., and Himo, F. 2007, J. Phys. Chem. B, 111, 1253.
62. Yang, Y., McCormick, J. M., and Solomon, E. I. 1997, J. Am. Chem. Soc., 119, 11832.
63. Smoukov, S. K., Quaroni, L., Wang, X., Doan, P. E., Hoffman, B. M., and Que, L. Jr. 2002, J. Am. Chem. Soc., 124, 2595.
64. Schenk, G., Elliott, T. W., Leung, E. W. W., Mitić, N., Carrington, L. E., Gahan, L. R., and Guddat, L. W. 2008, BMC Struct. Biol., 8, 6.
65. Aubert, S. D., Li, Y., and Raushel, F. M. 2004, Biochemistry, 43, 5707.
66. Leung, E. W. W., Teixeira, M., Guddat, L. W., Mitić, N., and Schenk, G. 2007, Curr. Topics Plant Biol., 8, 21.
67. Peracchi, A. 2001, Trends Biochem. Sci., 26, 497.
68. Wu, F., Li, W-S., Chen-Goodspeed, M., Sogorb, M. A., and Raushel, F. M. 2000, J. Am. Chem. Soc., 122, 10206.
69. Chen-Goodspeed, M., Sogorb, M. A., Wu, F., and Raushel, F. M. 2001, Biochemistry, 40, 1332.
70. Chen-Goodspeed, M., Sogorb, M. A., Wu, F., Hong, S-B., and Raushel, F. M. 2001, Biochemistry, 40, 1325.
71. Hong, S-B., and Raushel, F. M. 1999, Biochemistry, 38, 1159.
72. Castle, L. A., Siehl, D. L., Gorton, R., Patten, P. A., Chen, Y. H., Bertain, S., Cho, H.-J., Duck, N., Wong, J., Liu, D., and Lassner, M. W. 2004, Science, 304, 1151.
73. Reetz, M. T., Torre, C., Eipper, A., Lohmer, R., Hermes, M., Brunner, B., Maichele, A., Bocola, M., Arand, M., Cronin, A., Genzel, Y., Archelas, A., and Furstoss, R. 2004, Org. Lett., 6, 177.
74. Johannes, T. W., Woodyer, R. D., and Zhao, H. 2005, Appl. Environ. Microbiol., 71, 5728.
75. Liu, J-W., Hadler, K. S., Schenk, G., and Ollis, D. 2007, FEBS J., 274, 4742.

76. Petrounia, I. P., and Arnold, F. H. 2000, Curr. Opin. Biotechnol., 11, 325.
77. Arnold, F. H., and Volkov, A. A. 1999, Curr. Opin. Chem. Biol., 3, 54.
78. Johannes, T. W., and Zhao, H. 2006, Curr. Opin. Microbiol., 9, 261.
79. Kaur, J., and Sharma, R. 2006, Crit. Rev. Biotechnol., 26, 165.
80. Shimazu, M., Mulchandani A., Chen W. 2001, Biotechnol. Prog., 17, 76.
81. LeJeune, K. E., Wild, J. R., and Russell, A. J. 1998, Nature, 395, 27.
82. Richins, R. D., Kaneva, I., Mulchandani, A., and Chen, W. 1997, Nat. Biotech., 15, 984.
83. Cho, C. M. H., Mulchandani, A., and Chen, W. 2002, Appl. Environ. Microbiol., 68, 2026.
84. Cho, C. M. H., Mulchandani, A., and Chen, W. 2004, Appl. Environ. Microbiol., 70, 4681.
85. Griffiths, A. D., and Tawfik, D. S. 2003, EMBO J., 22, 24.
86. Briseno-Roa, L., Hill, J., Notman, S., Sellers, D., Smith, A. P., Timperley, C. M., Wetherell, J., Williams, N. H., Williams, G. R., Fersht, A. R., and Griffiths, A. D. 2006, J. Med. Chem., 49, 246.
87. Bernath, K., Hai, M., Mastrobattista, E., Griffiths, A. D., Magdassi, S., and Tawfik, D. S. 2004, Anal. Biochem., 325, 151.
88. McLoughlin, S. Y., Jackson, C., Liu, J-W., and Ollis, D. 2005, Protein Expr. Purif., 41, 433.